Sensors and Materials, Vol. 36, No. 5 (2024) 1787–1796
MYU Tokyo

S & M 3633

Preparation and Application of Rubber Fruit Shell Carbon as Decoration Material on ZnO for H_2S Gas Sensors

Rodiawan,[1] Sheng-Chang Wang,[1*] and Suhdi[2]

[1]Department of Mechanical Engineering, Southern Taiwan University of Science and Technology, No. 1 Nantai St., Yungkang Dist., Tainan City 710301, Taiwan
[2]Department of Mechanical Engineering, Bangka Belitung University, Desa Balunijuk Kec. Merawang, Kab. Bangka, Provinsi Kepulauan Bangka Belitung 33172, Indonesia

(Received October 26, 2023; accepted April 17, 2024)

Keywords: gas sensor, ZnO, rubber fruit shell carbon, room temperature

H_2S is a gas that can be hazardous to human health, even at low concentrations. Several studies have shown that people living near paper mills and oil and gas factories experience health problems and suffer from allergic reaction symptoms, including eye, nose, and respiratory symptoms in children and adults triggered by exposure to H_2S gas with concentrations of less than 100 ppb. In this study, we used biomass activated carbon produced from rubber fruit shells as a decoration material prepared with a chemical activating agent (KOH) with an impregnation ratio of 1:5. The process produces biomass activated charcoal with a carbon content of 79.05%. Then, 5% of the weight of the rubber fruit shell carbon was mixed with ZnO by a wet chemical process as a sensor material placed on a Au electrode. The sensing response was tested at H_2S concentrations of 20, 30, 40, 50, 60, 70, 80, 90, and 100 ppb at room temperature (25 °C). The results of the sensing response were 2.95, 4.60, 5.62, 5.94, 6.47, 6.62, 7.41, 8.84, and 10.00%, respectively. The research results showed that the ZnO gas sensor decorated with carbon can detect H_2S gas of less than 100 ppb. Additionally, this sensor can be operated at room temperature.

1. Introduction

Some gases generated by human activities contaminate the environment and are hazardous to human health. H_2S is a noxious gas that is colorless, odorless, corrosive, and highly toxic, and can be found in various industrial products, including natural gas, biogas, syngas, and petroleum.(1) When only a small amount of H_2S gas is released, it can irritate the nose and eyes and paralyze nerves. When a modest volume of this gas is inhaled, it can cause coughing, sore throat, and tightness in the chest. Moreover, an elevated H_2S gas concentration might result in symptoms such as headaches, impaired cognitive function, unconsciousness, and even death.(2) Although only a few studies have demonstrated the effects of exposure to a low concentration of H_2S, there was evidence of an impact of exposure to this gas in humans. The prolonged exposure of personnel in the Iranian petroleum industry to H_2S gas at concentrations ranging from 0 to 90

*Corresponding author: e-mail: scwang@stust.edu.tw
https://doi.org/10.18494/SAM4794

ISSN 0914-4935

ppb may adversely affect their health, according to Saeedi *et al.*[3] Kilburn and Warshaw found that residents living near the desulfurization unit of a California coastal refinery and exposed to 10 and 100 ppb H_2S at their peak had neurophysiological disorders.[4] The human olfactory threshold for H_2S is between 10 and 300 ppb, depending on individual sensitivity.[5] In this study, we fabricated a gas sensor that can detect H_2S within the above concentration range.

Over the last decade, MOSs have become the most popular materials for sensing gases at low concentrations. Young and Chu prepared zinc oxide nanorods (ZnO NRs) decorated with platinum nanoparticles (Pt NPs) using DC magnetron sputtering. The gas sensors' results are consistent, stable, and repeatable. The sensitivity was 121.03%.[6] The sputtering process was carried out for 0 and 30 s. The ZnO and Pt/ZnO NR sensor gas materials show consistent, stable, and repeatable behavior. The ZnO and Pt/ZnO NR sensors have sensitivities of 1.34 and 121.03%, respectively, at a methanol gas concentration of 1000 ppm and an operating temperature of 270 °C.[6] Lee *et al.* reported that Pd-functionalized 0.1 In_2O_3-loaded ZnO nanofibers showed a robust reaction to 50–152 ppb H_2 gas at 350 °C.[7] Wu and Akhtar concluded that sensors based on the nanocomposites of 5 wt% MoS_2-ZnO-Zn_2SnO_4 have a limit of detection of 0.05–2 ppm for H_2S gas at 30 °C.[8] Fu *et al.* discovered that the SnO_2/ZnO hetero-nanostructure can detect 10 ppb H_2S at 100 °C.[9] From the abovementioned research, ZnO is the material of choice because it can detect gas concentrations up to ppb levels. In addition, ZnO is a metal with unique properties as a gas sensor material, such as being an n-type II-VI semiconductor with a broad bandgap (3.37 eV), a large excitation binding energy (60 meV), and a high electron mobility [400 $cm^2/(V{\cdot}s)$].[10] The gas sensor that operates at room temperature is preferred because it is cheaper to operate. Various studies on sensors that operate at room temperature have been carried out. Su and Chai reported that the unique catalytic and electronic characteristics of Ag nanowires (NWs) can enhance the response of H_2S gas sensors at room temperature at ppb concentration levels by adding Ag NWs made from hollow Ag NW/PPy NT nanocomposites.[11] The ZnO/CuO composite made on the basis of bimetallic metal organic frameworks, using the hydrothermal synthesis of ZnO/CuO (Cu:Zn = 1:0.33), has a performance of 393.35 with a H_2S concentration of 10 ppm at temperatures up to 40 °C.[12] A gas sensor based on the MoS_2/SWCNT material presented high selectivity, performance, and responsiveness, and a short recovery time at ambient temperature.[13] The detection of NO_2 gas in ppm measured at room temperature showed better sensitivity and recovery time with MoS_2/CNT samples than with pure CNT.[14] The growth of high-density CNTs on an oxidized Si substrate by a simple method was applied to the direct transfer of high-density CNTs from a SiO_2/Si substrate to a flexible substrate for the fabrication of a CNT-based gas sensor as an ethanol gas sensing device operable with high sensitivities of 1.67 and 5.39% at room temperature.[15,16] On the basis of this explanation, carbon was chosen because it can be used to decorate the primary material of sensors operating at room temperature. Additionally, carbon possesses exceptional attributes, including high sensitivity, long-term stability, a high-quality crystal lattice, high carrier mobility (such as ballistic charge transport), and low noise.[17] Biomass activated carbon should be used as the sensing material because of its low cost, renewability, minimal ash content, and low environmental impact

compared with traditionalactivated carbon.[18] A wide range of biomass materials have been examined, such as coconut shells, cashew shells, rice husks, durian skin, sugarcane debris, maize crops, potato starch, and banana skin. However, these materials have a low carbon content, a high volume-to-weight ratio, and a significant ash component.[19] Therefore, biomass activated carbon from rubber fruit shells was demonstrated as a decoration material as it is inexpensive and abundant and has a high carbon content.

In this study, we used ZnO as the main material and biomass activated carbon from rubber fruit shells as the decoration material to be tested at the operating temperature of 25 ℃. Sensor performance measurements were carried out at H_2S concentrations of 20, 30, 40, 50, 60, 70, 80, 90, and 100 ppb.

2. Materials and Methods

ZnO powder (nanopowder <100 nm, Sigma-Aldrich, USA) and rubber fruit shells were used to produce biomass activated carbon, as shown in Fig. 1. To obtain the activated carbon, we soaked rubber fruit shells in a bucket containing 10% H_2SO_4 for 24 h, then rinsed them with DI water to remove stuck dirt, followed by drying in an oven at 60 ℃ for 24 h. After that, we put the dried precursor into a furnace and carbonized it at 450 ℃ for 1 h under nitrogen ambient (with a flow rate of 20 mL/min). After that, the carbonized rubber fruit shells were crushed and filtered using a 200 mesh/74 μm sieve. The active ingredient is a 50% KOH solution mixed with 3 g of rubber fruit shell powder with an impregnation ratio of 1:5. The slurry was stirred at 1000 rpm for 90 min until a uniform mixture was obtained. Then, we dried it in an oven at 110 ℃ overnight. Next, we heated the dried mixture at 450 ℃ for 30 min, then at 800 ℃ for 120 min. The resulting activated carbon was washed several times with 1 M HCl and distilled water to remove any remaining activation agent residue. Finally, we dried the activated carbon in an oven at 110 ℃ for 24 h.[19]

C-ZnO was prepared by wet chemistry.[20] The deposition solution of C-ZnO on the electrode was prepared by drop casting methods.[21] Both 10 mg of ZnO and 0.5 mg of carbon NPs were mixed with 10 ml of DI water under ultrasonication. After thorough mixing, we dropped 2 μl of slurry onto the electrode, then dried it at 50 ℃ in the furnace overnight. Finally, C-ZnO was deposited on Au electrodes, as shown in Fig. 2, followed by annealing at 500 ℃ for 10 min.

The performance of gas sensor devices was determined by gas chamber measurement with a syringe at H_2S concentrations of 20, 30, 40, 50, 60, 70, 80, 90, and 100 ppb. The sensing response is the air current minus the gas current divided by the gas current multiplied by 100%, as presented in Eq. (1).[22] The measurement was conducted at 25 ℃, which corresponds to room temperature.

$$S = \frac{R_a - R_g}{R_g} \times 100\% \tag{1}$$

Structural and morphological observations of the material were carried out using SEM, TEM, and XRD.

Fig. 1. (Color online) Rubber fruit shells.

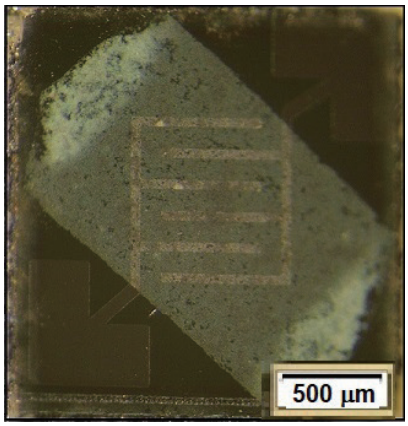

Fig. 2. (Color online) C-ZnO material deposited on Au electrodes.

3. Experimental Results

The XRD graph of the biomass activated carbon from rubber fruit shells, as shown in Fig. 3, shows that the biomass activated carbon is amorphous. The structure of biomass activated carbon corresponds to the (002) and (001) planes and the broad peak is at 2θ = 27 and 44°. Crystallites are created through the stacking of two or more plates. A crucial characteristic of a well-characterized adsorbent, such as activated carbon, is the lack of distinct peaks, which suggests that it has a primarily amorphous structure.[23]

The rubber fruit shell carbon particles were simple, uniform agglomerations. Such agglomerations are spread across the surface, as shown in Fig. 4(a). The particle size varied with a minimum diameter of 14 nm, a maximum diameter of 159 nm, and a mean diameter of 72.123 nm, as presented in Fig. 4(b).

The element analysis of rubber fruit shell carbon shows that Si and P have similar atomic weights of 0.32%, followed by K with an atomic weight of 2.38% and two other elements with high atomic weights, namely, oxygen and carbon, with their compositions of 17.93 and 79.05%, respectively, as presented in Fig. 5.

The XRD pattern shown in Fig. 6 is that of C-ZnO annealed at 500 °C. The diffraction peaks of ZnO are at the angles of 31.43, 34.10, 35.93, 47.32, 56.38, 62.94, 66.46, 68.06, and 69.20°, which correspond to the ZnO peaks from (100), (002), (101), (102), (110), (103), (200), (112), and (201) planes, respectively. The carbon peaks are also revealed with the same peak planes and angular numbers as in Fig. 3. In this picture, there is also a ZnC peak at an angle of 38.28°.[24]

It can be observed that spherical ZnO and C grains are spread with relatively the same size, as shown in Fig. 7. Moreover, we characterized the carbon grains between the ZnO grains, by comparing the two TEM images in Figs. 8(a) and 8(b). C grains appear brighter and more fibrous, as shown in Fig. 8(b).

The EDS structural spectrum of C-ZnO shows that Zn has an atomic weight of 33.04%, followed by O with the highest atomic weight of 41.28%. C has an atomic weight of 21.71%, and two other elements, Si and P, have atomic weights of 2.90 and 1.07%, respectively, as shown in Fig. 9.

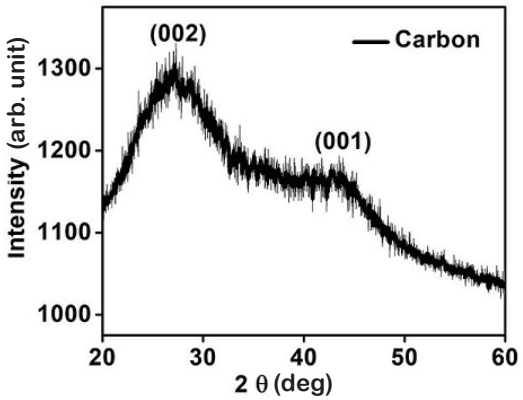

Fig. 3. XRD pattern of biomass activated carbon.

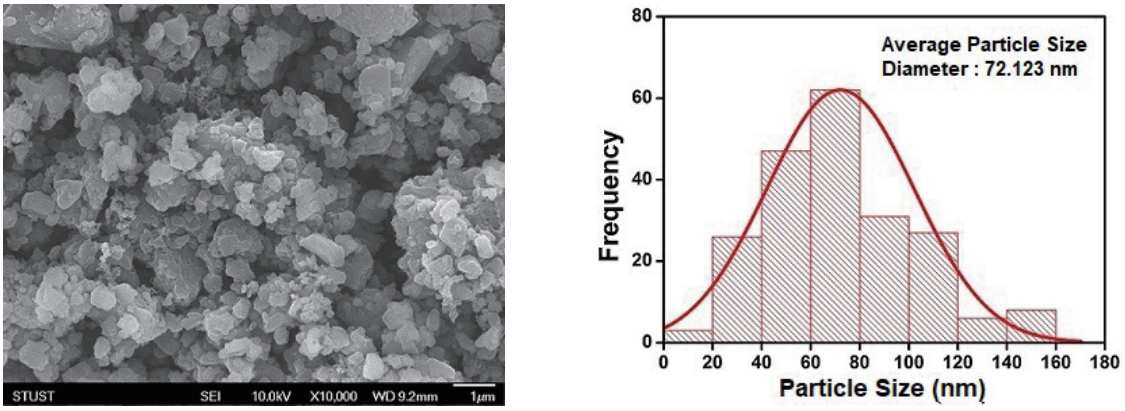

(a) (b)

Fig. 4. (Color online) (a) SEM image of surface of biomass activated carbon. (b) Grain size distribution histogram curve of biomass activated carbon.

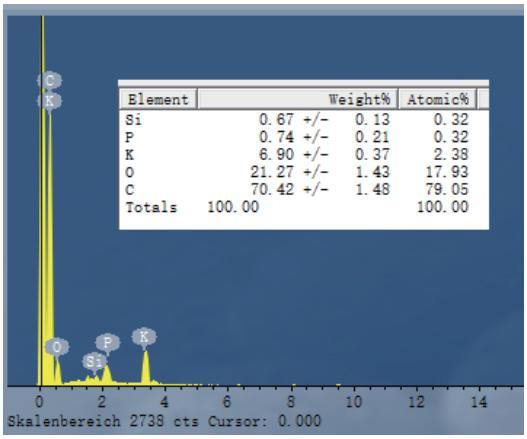

Fig. 5. (Color online) EDS spectrum of biomass activated carbon.

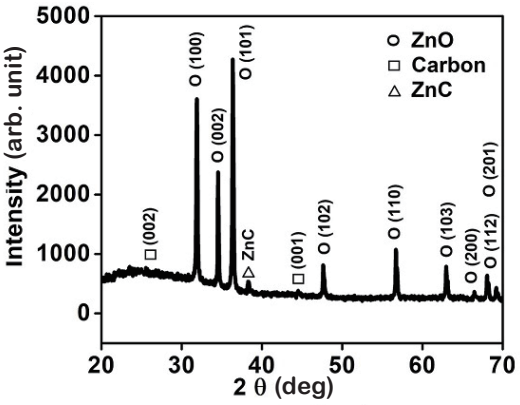

Fig. 6. XRD pattern of C-ZnO.

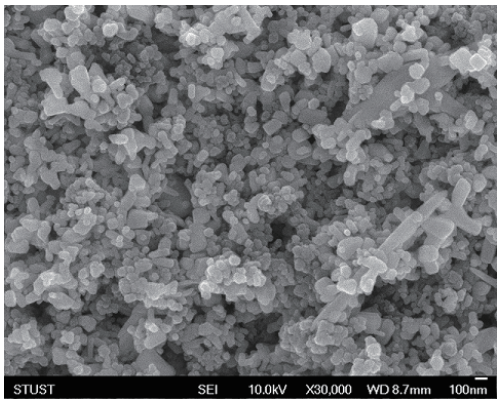

Fig. 7. SEM image of surface C-ZnO.

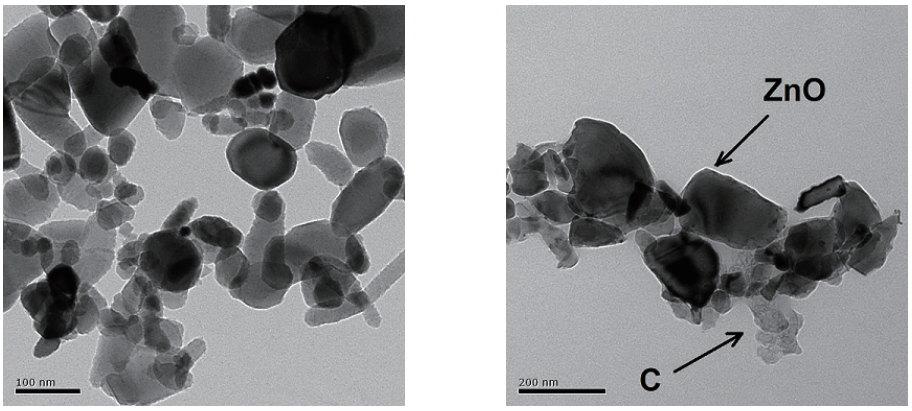

(a) (b)

Fig. 8. (a) TEM images of ZnO and (b) surface C-ZnO.

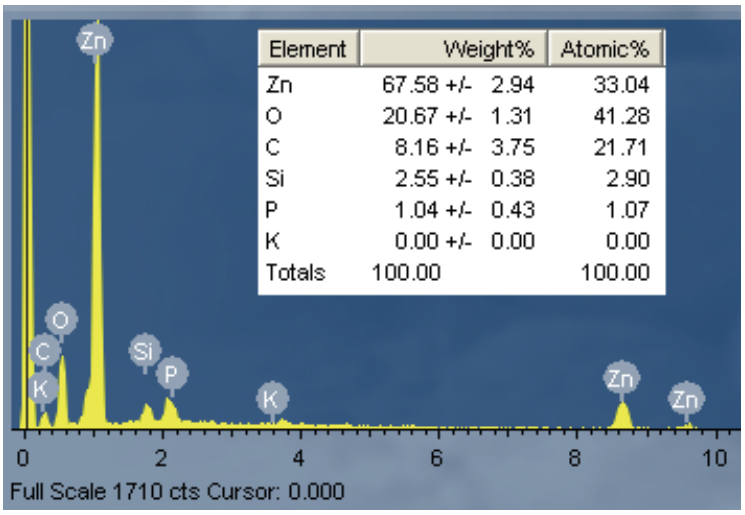

Fig. 9. (Color online) EDS spectrum of C-ZnO.

The sensing response was determined at H_2S concentrations of 20, 30, 40, 50, 60, 70, 80, 90, and 100 ppb and 25 °C. These results are quite good for the ppb concentrations with sensitivities of 2.95, 4.60, 5.62, 5.94, 6.47, 6.62, 7.41, 8.84, and 10.00%, respectively, as shown in Fig. 10. The measurement results reveal that the C-ZnO sensor can still detect H_2S gas even at a low concentration that affects human health.

Response time is defined as the increase in the percentage of sensing response measured from zero until there is no further increase; then, the percentage of sensing response tends to plateau. In contrast, recovery time is defined as the decrease in the percentage of sensing response from the highest point to zero. The shock effect of the cessation of gas exposure causes the increase in the percentage of sensing response at the peak in the image. In this study, the response time was about 71 s, whereas the recovery time was about 85 s, as shown in Fig. 11.

When exposed to oxygen, the C-ZnO sensor surface will react with oxygen molecules, as indicated by Eqs. (2)–(4);[25] oxygen molecules will capture electrons flowing in the C-ZnO material and a thick depletion layer will form, which will increase the resistance. When the surface of the C-ZnO sensor is exposed to H_2S gas, oxygen molecules will react with S and form SO_2, as indicated by Eq. (5),[26] and release back electrons; then, the depletion layer will become thinner and the resistance will decrease,[27] as shown in Fig. 12.

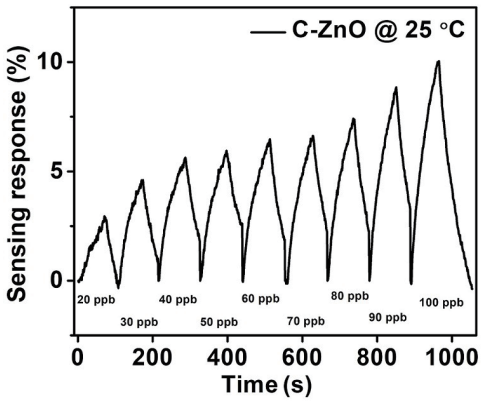

Fig. 10. Sensing response of C-ZnO for H_2S at 25 °C.

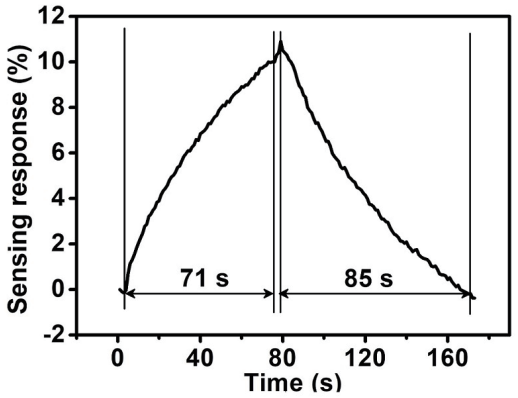

Fig. 11. Response and recovery times of C-ZnO for H_2S at 25 °C.

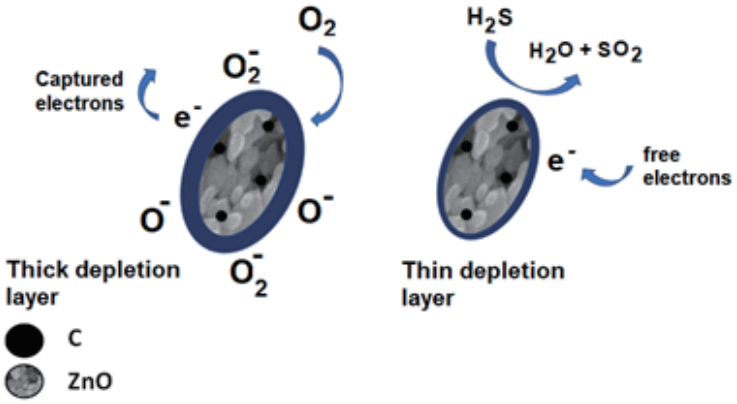

Fig. 12. (Color online) Sensing mechanism.

Table 1
Comparison of H_2S gas sensing responses from different studies and this study.

Material	Concentration	Temperature (°C)	Response (%)	Response and recovery times (s)	Reference
Cu_2O/CuO-decorated MWCNTs	1–5 ppm	150	1613	219 and 77	(29)
SnO_2/rGO/PANI	50 ppb–50 ppm	Room temp.	9.1 (100 ppb)	—	(30)
PPy/WO_3	100–1000 ppb	Room temp.	8.9 (100 ppb)	6 and 210	(31)
WO_3 nanoflake array film	0.1–10 ppm	100-300	2.8 up to 85	—	(32)
CuO/SWCNTs	0.1–50 ppm	150	6 (100 ppb)	—	(33)
C-ZnO	20-100 ppb	Room temp.	2.95–10	71 and 85	This study

$$O_2\ (gas) \rightarrow O_2\ (ads) \tag{2}$$

$$O_2\ (ads) + e^- \rightarrow O_2^-\ (ads) \tag{3}$$

$$O_2^-\ (ads) + e^- \rightarrow 2O^-\ (ads) \tag{4}$$

$$H_2S + 3O^-\ (ads) \rightarrow H_2O + SO_2 + 3e^- \tag{5}$$

The carbon nanoparticle material plays a role in the sensor operating at room temperature. Franco *et al*. reported that carbon materials such as carbon nanotubes, graphene, carbon black, and carbon nanofibers have many advantages, such as good stability, electrical conductivity, and surface defect sites that can be created when used in nanocomposites with other materials. When utilized with metal oxides, this carbon material proves to be very promising for developing highly sensitive sensing platforms at room temperature.[28]

Table 1 shows the performance of the H_2S gas sensor with several different materials. Most studies used different materials, which are then used to measure H_2S at a concentration of 100 ppb; almost all of them produced similar sensing responses. However, our study showed slightly higher results. Apart from that, the recovery of C-ZnO is slightly faster than that of PPY/WO_3, namely, 85 s for C-ZnO and 210 s for PPY/WO_3. Therefore, C-ZnO is suitable for low-concentration H_2S gas sensors.

4. Conclusions

In this study, we made biomass activated carbon from rubber fruit shells with a carbon content of 79.05%. SEM surface image results revealed that the carbon grain size varies with a minimum diameter of 14 nm, a maximum diameter of 159 nm, and an average diameter of 72.123 nm. The EDS structural spectrum of 0.5 mg of biomass activated carbon mixed with 10 mg of ZnO produces a composition of Zn of 33.04% atomic weight and O of 41.28% atomic weight. The atomic weight of carbon is 21.71%, that of Si is 2.90%, and those of P are 2.90 and 1.07%. The sensor material of ZnO decorated with biomass activated carbon can detect H_2S at concentrations of 20, 30, 40, 50, 60, 70, 80, 90, and 100 ppb at 25 °C with results of 2.95, 4.60,

5.62, 5.94, 6.47, 6.62, 7.41, 8.84, and 10.00%, respectively. On the basis of these results, we suggest that biomass activated carbon created from rubber fruit shells can be used as a decoration material to obtain a sensitive sensing response and decrease the operation temperature of the gas sensor.

Acknowledgments

We thank the ROC Ministry of Science and Technology for providing financial support for this research, as outlined in Grant No. NSTC 112-2221-E-218-007.

References

1 T. Yu, Z. Chen, Z. Liu, J. Xu, and Y. Wang: Separations **9** (2022) 229. https://doi.org/10.3390/separations9090229
2 J. Sheoran and R. Kumar: J. Phys. Conf. Ser. **2267** (2022) 012008. https://doi.org/10.1088/1742-6596/2267/1/012008
3 A. Saeedi, A. Najibi, and A. M. Bardbori: Int. J. Occup. Environ. Med. **6** (2015) 20. https://pubmed.ncbi.nlm.nih.gov/25588222/
4 K. H. Kilburn and R. H. Warshaw: Toxicol. Ind. Health **11** (1995) 185. https://doi.org/10.1177/074823379501100206
5 T. L. Guidotti: Int. J. Toxicol. **29** (2010) 569. https://doi.org/10.1177/1091581810384882
6 S. J. Young, and Y. L. Chu: J Electrochem Soc. **167** (2020) 147508. https://doi.org/10.1149/1945-7111/abc4be
7 J. H. Lee, J. H. Kim, J. Y. Kim, A. Mirzaei, H. W. Kim, and S. S. Kim: Sensors **19** (2019) 1. https://doi.org/10.3390/s19194276
8 D. Wu and A. Akhtar: Molecules **28** (2023) 3230. https://doi.org/10.3390/molecules28073230
9 D. Fu, C. Zhu, X. Zhang, C. Li, and Y. Chen: J. Mater. Chem. A **4** (2016) 1390. https://doi.org/10.1039/C5TA09190J
10 Y. Kang, F. Yu, L. Zhang, W. Wang, L. Chen, and Y. Li: Solid State Ionics **360** (2021) 115544. https://doi.org/10.1016/j.ssi.2020.115544
11 P. G. Su and X. C. Chai: Chemosensors **10** (2022) 305. https://doi.org/10.3390/chemosensors10080305
12 X. Wang, S. Li, L. Xie, X. Li, D. Lin, and Z. Zhu: Ceram. Int. **46** (2020) 15858. https://doi.org/10.1016/j.ceramint.2020.03.133
13 H. Rhyu, S. Lee, M. Kang, D. Yoon, S. Myung, W. Song, S. S. Lee, and J. Lim: RSC Adv. **13** (2023) 13128. https://doi.org/10.1039/D3RA01183F
14 G. Deokar, P. Vancsó, R. Arenal, F. Ravaux, J. C. Cháfer, E. Llobet, A. Makarova, D. Vyalikh, C. Struzzi, P. Lambin, M. Jouiad, and J. F. Colomer: Adv. Mater. Interfaces **4** (2017) 1. https://doi.org/10.1002/admi.201700801
15 S. J. Young and Z. D. Lin: Microsyst. Technol. **24** (2018) 55. https://doi.org/10.1007/s00542-016-3154-2
16 S. J. Young and Z. D. Lin: ECS J. Solid State Sci. Technol. **6** (2017) M130. https://doi.org/10.1149/2.0211710jss
17 E. Llobet: Sens. Actuators, B **179** (2013) 32. https://doi.org/10.1016/j.snb.2012.11.014
18 P. Feng, J. Li, H. Wang, and Z. Xu: ACS Omega **5** (2020) 24064. https://doi.org/10.1021/acsomega.0c03494
19 Suhdi and S. C. Wang: Appl. Sci. **11** (2021) 3994. https://doi.org/10.3390/app11093994
20 I. S. Hwang, Y. S. Kim, S. J. Kim, B. K. Ju, and J. H. Lee: Sens. Actuators, B **136** (2009) 224. https://doi.org/10.1016/j.snb.2008.10.042
21 M. I. Nemufulwi, H. C. Swart, and G. H. Mhlongo: Processes **9** (2021) 1. https://doi.org/10.3390/pr9101791
22 S. Haviar, S. Chlupová, P. Kúš, M. Gillet, V. Matolín, and I. Matolínová: Int. J. Hydrogen Energy **42** (2017) 1344. https://doi.org/10.1016/j.ijhydene.2016.09.187
23 H. A. Zakaria, W. S. W. Mansor, and N. Shahrin: MATTER: Int. J. Sci. Technol. **3** (2018) 240. https://doi.org/10.20319/MIJST.2018.33.240252
24 D. K. Mishra, J. Mohapatra, M. K. Sharma, R. Chattarjee, S. K. Singh, S. Varma, S. N. Behera, S. K. Nayak, and P. Entel: J. Magn. Magn. Mater. **329** (2013) 146. https://doi.org/10.1016/j.jmmm.2012.09.058
25 C. Wang, L. Yin, L. Zhang, Y. Qi, N. Lun, and N. Liu: Langmuir **26** (2010) 12841. https://doi.org/10.1021/la100910u
26 F. N. Meng, X. P. Di, H. W. Dong, Y. Zhang, C. L. Zhu, C. Li, and Y. J. Chen: Sens. Actuators, B **182** (2013) 197. https://doi.org/10.1016/j.snb.2013.02.112

27 J. Kim and K. Yong: J. Phys. Chem. C **115** (2011) 7218. https://doi.org/10.1021/jp110129f
28 M. A. Franco, P. P. Conti, R. S. Andre, and D. S. Correa: Sens. Actuators Rep. **4** (2022) 100100. https://doi.org/10.1016/j.snr.2022.100100
29 J. H. Bang, A. Mirzaei, M. S. Choi, S. Han, H. Y. Lee, S. S. Kim, and H. W. Kim: Sens. Actuators, B **344** (2021) 130176. https://doi.org/10.1016/j.snb.2021.130176
30 D. Zhang, Z. Wu, and X. Zong: Sens. Actuators, B **289** (2019) 32. https://doi.org/10.1016/j.snb.2019.03.055
31 P. G. Su and Y. T. Peng: Sens. Actuators, B **193** (2014) 637. https://doi.org/10.1016/j.snb.2013.12.027
32 S. Poongodi, P. S. Kumar, D. Mangalaraj, N. Ponpandian, P. Meena, Y. Masuda, and C. Lee: J. Alloys Compd. **719** (2017) 71. https://doi.org/10.1016/j.jallcom.2017.05.122
33 M. Asad and M. H. Sheikhi: Sens. Actuators, B **231** (2016) 474. https://doi.org/10.1016/j.snb.2016.03.021

About the Authors

Rodiawan received his B.S. degree from Sriwijaya University, Indonesia, in 2000 and his M.S. degree from Wollongong University, Australia, in 2007. From 2007 to 2019, he was an assistant professor at Bangka Belitung University (UBB), Indonesia. Since 2019, he has been a Ph.D. student at Southern Taiwan University of Science and Technology, Taiwan. His research interests are in nanomaterials and gas sensors. (da71y208@stust.edu.tw)

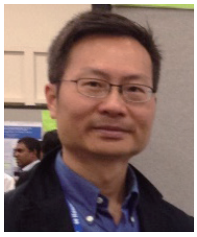

Sheng-Chang Wang received his B.S. degree from Feng Chia University, Taiwan, in 1992 and his M.S. and Ph.D. degrees from National Taiwan University, Taiwan, in 1997 and 2001, respectively. From 2014 to 2018, he was a professor and the Director of the Nanotechnology Research Center at Southern Taiwan University of Science and Technology, Taiwan. Since 2018, he has been a professor and the Chairman of the Department of Mechanical Engineering of Southern Taiwan University of Science and Technology, Taiwan. His research interests are in nanomaterials for energy applications, ceramic processing, TEM analyses, and electrophoretic deposition. (scwang@stust.edu.tw)

Suhdi received his B.S. degree from Polman Bandung, Indonesia, in 2001, his M.S. degree from ITB, Indonesia, in 2009, and his Ph.D. degree from Southern Taiwan University of Science and Technology, Taiwan, in 2021. He has been a lecturer in the Mechanical Engineering study program of Bangka Belitung University (UBB) since 2006 and an assistant professor since 2011. His research interests are in the microporous structures of carbonaceous materials, carbon nanomaterials and applications, and biomass composite materials. (suhdi@ubb.ac.id)